Self-Assembly

DOI: 10.1002/ange.201309680

# Gated Electron Sharing Within Dynamic Naphthalene Diimide-Based Oligorotaxanes**

*Alyssa-Jennifer Avestro, Daniel M. Gardner, Nicolaas A. Vermeulen, Eleanor A. Wilson, Severin T. Schneebeli, Adam C. Whalley, Matthew E. Belowich, Raanan Carmieli, Michael R. Wasielewski,* and J. Fraser Stoddart**

***Abstract:*** *The controlled self-assembly of well-defined and spatially ordered π-systems has attracted considerable interest because of their potential applications in organic electronics. An important contemporary pursuit relates to the investigation of charge transport across noncovalently coupled components in a stepwise fashion. Dynamic oligorotaxanes, prepared by template-directed methods, provide a scaffold for directing the construction of monodisperse one-dimensional assemblies in which the functional units communicate electronically through-space by way of π-orbital interactions. Reported herein is a series of oligorotaxanes containing one, two, three and four naphthalene diimide (NDI) redox-active units, which have been shown by cyclic voltammetry, and by EPR and ENDOR spectroscopies, to share electrons across the NDI stacks. Thermally driven motions between the neighboring NDI units in the oligorotaxanes influence the passage of electrons through the NDI stacks in a manner reminiscent of the conformationally gated charge transfer observed in DNA.*

Electron transport has been shown to play a crucial role in the functioning of biological systems,[1] light-harvesting cascades,[2] molecular actuators and switches,[3] and polymeric materials.[4] Understanding how electrons move from one molecular component to the next over long discrete distances remains an important goal in the development of nanomaterials for organic molecular electronics. Covalent donor-bridge-acceptor (D-B-A) systems have been used extensively[5] to 1) demonstrate charge transport in one-dimensional (1D) systems having well-defined D–A distances and orientations, and 2) expand our knowledge of how molecular structure and dynamics impact charge-transfer processes. Electron or hole transport within covalent D-B-A molecules is most often *through-bond*,[6] whereas transport in self-assembled noncovalent D-B-A systems is generally *through-space*.[7]

Many approaches[8–12] to the fabrication of through-space "molecular wire" systems with discrete architectures often require elegant, multi-step syntheses. Alternative strategies make use of less complex covalent building blocks that self-assemble into oligomers having relatively low polydispersities[9] as well as template-directed methods[10] to control the self-assembly of planar aromatics into 1D architectures.[11] For example, Wu et al.[12] have used G-quadruplexes to construct discrete assemblies of electron and hole charge carriers, while Matile et al.[13] have established a general bottom-up method for effecting the template-directed, self-organizing surface initiated polymerization (SOSIP) of functional monomers into vertical multicomponent photosystems. By relying on a combination of hydrogen bonding, π–π stacking and reversible ring-opening polymerization, oriented long-range photoactive layers can be produced on indium tin oxide (ITO) surfaces with low polydispersities. Meanwhile, Fujita et al.[14a] have combined the host-guest chemistry of columnar Pd-coordination cages with the direct binding nanogap technique developed by Kiguchi and co-workers[15] in order to obtain conductance measurements on molecular junctions composed of discretely assembled π-stacks containing four, five, and six aromatic units.[14b] In this case, the number of aromatic guests in the stack is pre-determined by the length and size of the host, the initial preparation of which is limited by the availability of appropriately long and/or rigid ligands. Recently, we capitalized upon a highly efficient template-

[*] A.-J. Avestro, D. M. Gardner, Dr. N. A. Vermeulen, E. A. Wilson, Dr. S. T. Schneebeli, Dr. A. C. Whalley, Dr. M. E. Belowich, Prof. R. Carmieli, Prof. M. R. Wasielewski, Prof. J. F. Stoddart
Center for the Chemistry of Integrated Systems (CCIS) and Argonne-Northwestern Solar Energy Research (ANSER) Center
Department of Chemistry, Northwestern University
2145 Sheridan Road, Evanston, IL 60208 (USA)
E-mail: m-wasielewski@northwestern.edu
stoddart@northwestern.edu
Homepage: http://chemgroups.northwestern.edu/wasielewski
http://stoddart.northwestern.edu

[**] We would like to thank Dr. Saman Shafaie for collecting high-resolution mass spectrometric data, Drs. Charlotte Stern and Amy A. Sargeant for single-crystal structure determination, and Drs. James M. Holcroft and Marco Frasconi for helpful discussions. This research is part (Project 34-947) of the Joint Center of Excellence in Integrated Nano-Systems (JCIN) at King Abdul-Aziz City for Science and Technology (KACST) and Northwestern University (NU). We would like to thank both KACST and NU for their continued support of this research. M.R.W. is supported by the Chemical Sciences, Geosciences, and Biosciences Division, Office of Basic Energy, DOE, under grant no. DE-FG02-99ER-14999. A.-J.A. gratefully acknowledges the National Science Foundation (NSF) for the award of a Graduate Research Fellowship (GRF) under Grant No. DGE-0824162. D.M.G. was supported by the Department of Defense through the National Defense Science & Engineering Graduate Fellowship (NDSEG) Program. S.T.S. thanks the International Institute for Nanotechnology (IIN) at NU for an IIN Postdoctoral Fellowship and the QUEST high-performance computing center at NU for a research allocation of computer time. R.C. is supported by the ANSER Center, an Energy Frontier Research Center funded by the U.S. Department of Energy, Office of Science, Office of Basic Energy Sciences under Award Number DE-SC0001059.

Supporting information for this article is available on the WWW under http://dx.doi.org/10.1002/anie.201309680.

  

directed clipping strategy[16] utilizing the concept of dynamic covalent chemistry[17] (DCC) to prepare a series of rigid oligorotaxanes[18] featuring a precise number of [24]crown-8 rings which encircle an oligoammonium dumbbell containing ***x*** $-(CH_2CH_2NH_2^+CH_2)-$ recognition sites spaced 3.4 Å apart, an ideal distance for sustaining π–π stacking interactions. These oligorotaxanes can be isolated in near quantitative yields (up to 96%) in $<10$ min at room temperature. Employing this same approach, we envisioned the self-assembly of redox-active units into ordered 1D arrays for the systematic investigation of through-space electron transport over well-defined distances. Here we report 1) the application of DCC in the preparation of *n*-type single-molecular arrays, featuring electron-deficient naphthalene diimides and 2) the utility of mechanically interlocked architectures in the broader development of organic electronic materials, while at the same time assessing 3) the influence of the mechanical bond, that is, the dynamic nature of the rotaxane components, on electron transfer.

Herein, we describe the synthesis and intramolecular electron sharing properties of a new series (Scheme 1) of oligorotaxanes **[*n*]NDI$_x$R** featuring one, two, three, and four rings (i.e., ***x*** = 1–4)—functionalized with naphthalene diimide (NDI)—which encircle oligoammonium dumbbells **D*x*** where ***x*** also represents the number of $-(CH_2CH_2NH_2^+CH_2)-$ recognition sites for the rings. NDI is an attractive functional unit because of 1) its large π-surface, 2) its propensity to self-assemble into co-facial stacks, 3) its excellent photochemical/thermal stability, 4) its predictable *n*-type redox behavior and 5) its electronic tenability via naphthalene core substitution methods, making it a suitable candidate for fundamental investigations of charge and energy transfer processes.[19] Soluble NDI derivatives are also easily prepared and modified by attaching substituents to the diimide nitrogens without affecting their electronic properties.[20] The oligorotaxanes **[*n*]NDI$_x$R** were prepared by mixing ***x*** equivalents each of the acyclic precursor **1-NDI** and tetraethylene glycol bis(2-aminophenyl)ether (**2**) in the presence of 1.0 equiv of the dumbbell **D*x*** using the clipping procedure.[16,18] For more details, see the Experimental Section and Scheme S6 in the Supporting Information. A control NDI derivative **3** was also prepared for comparison. All of the compounds were fully characterized by $^1$H and $^{13}$C NMR spectroscopies, as well as by high-resolution electron-spray ionization (HR-ESI) mass spectrometry (Supporting Information, Sections 2 and 3). The crude $^1$H NMR spectra (Figure 1) of the [2]-, [3]-, [4]-, and

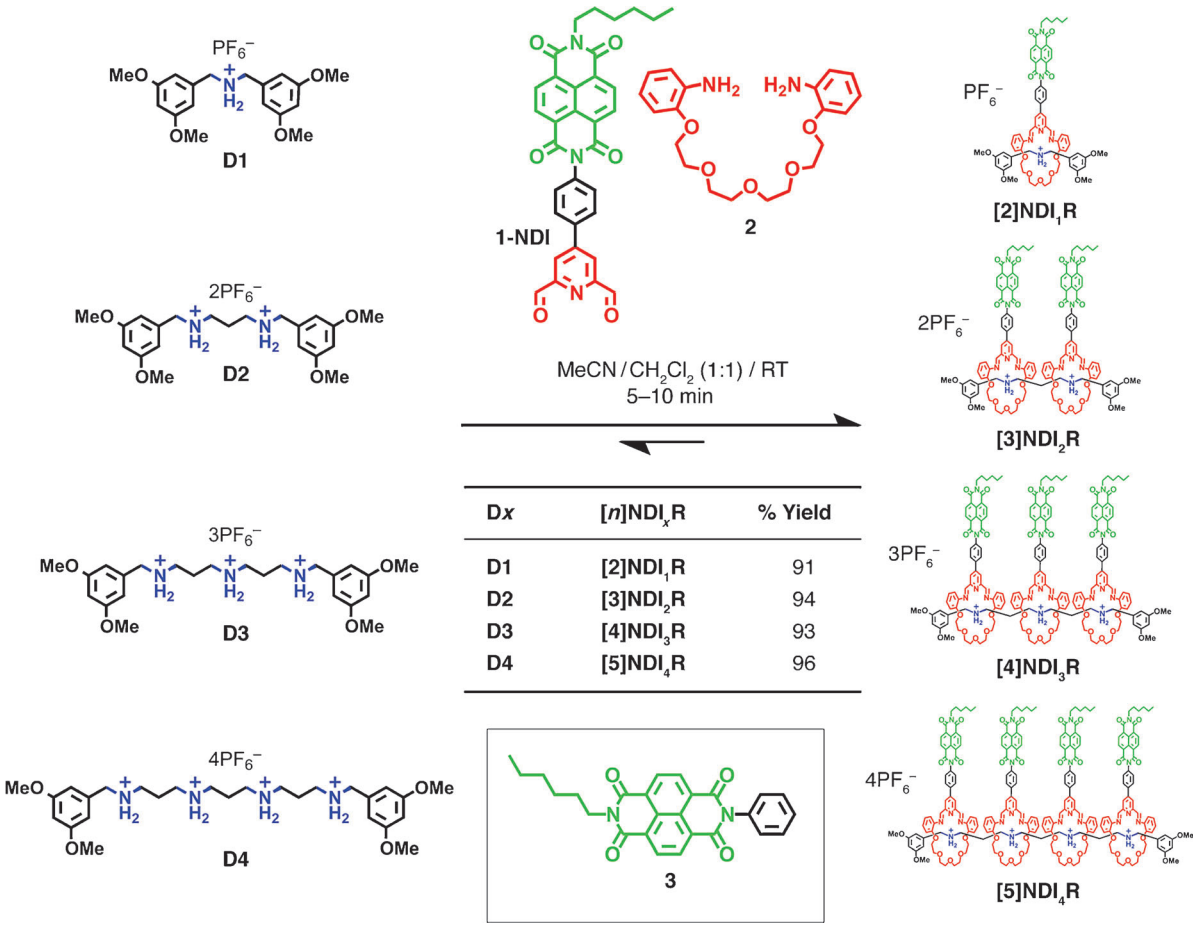


| D*x* | [*n*]NDI$_x$R | % Yield |
|---|---|---|
| D1 | [2]NDI$_1$R | 91 |
| D2 | [3]NDI$_2$R | 94 |
| D3 | [4]NDI$_3$R | 93 |
| D4 | [5]NDI$_4$R | 96 |

***Scheme 1.*** Synthesis of the **[*n*]NDI$_x$R** series starting from 1.0 equiv of an oligoammonium dumbbell **D*x*** (where ***x*** = 1, 2, 3, or 4) and ***x*** equiv of acyclic clipping precursors **1-NDI** and **2** to afford the thermodynamically controlled self-assembly of [2]-, [3]-, [4]-, and [5]rotaxanes containing one, two, three, and four NDI units, respectively. The constitutionally unsymmetrical NDI derivative **3** was prepared to in order to serve as a control compound.

[5]rotaxanes reveal that, in all cases, the oligorotaxanes are formed quantitatively in < 10 min, demonstrating the power of the clipping methodology for the production of assemblies with precise control in an efficient manner. The resonances for the NDI protons, $H_a$ and $H_b$, in **[2]NDI$_1$R** appear (Figure 1a) as a "tight" AB system centered around 8.80 ppm despite the asymmetry of the NDI unit, whereas for **[3]NDI$_2$R**, the signals for the same protons separate (Figure 1b) into a well-defined AX system ($\delta = 8.40$, 8.20 ppm) indicative of π–π stacking interactions between the NDI units. This separation is exaggerated even more so in the spectra (Figure 1c,d) of **[4]NDI$_3$R** and **[5]NDI$_4$R**. In agreement with the literature[18] the resonances for the imine and aromatic protons shift towards higher and higher fields as the number of rings increase.[21]

Since growing single crystals of ***[n]*NDI$_x$R** suitable for X-ray diffraction analysis has so far evaded us,[22] we focused our attention on quantum mechanical modeling, starting from the crystal structure (Figure 2a; see also the Supporting Information, Section 4) of the related [3]rotaxane[23] **[3]Ph$_2$R** which is devoid of NDI units *para*-substituted on the Ph rings. Density functional calculations[24,25] of **[3]NDI$_2$R** afforded (Figure 2b) the two parallel-aligned NDI units with an average plane-to-plane separation of 3.4 Å and an NDI-$C_6H_4$ dihedral angle of 59°. Populating the molecule with an additional single electron to form the mono-reduced radical anion **([3]NDI$_2$R)$^{\bullet-}$** generates a SOMO (Figure 3) spanning both NDI units which suggests that the unpaired electron is shared within the [3]rotaxane. On the other hand, variable-temperature (VT) $^1$H NMR spectra (Supporting Information, Section 3.2) for the [3]-, [4]-, and [5]rotaxanes show slight broadening of the resonances for the NDI protons ($H_a$ and $H_b$) as the temperature is decreased, whereas the signals for these same protons in the [2]rotaxane **[2]NDI$_1$R** remain sharp. This observation implies interconversion between various co-conformations of the NDI-appended rings on the $^1$H NMR timescale at 298 K, as well as an increase in the population of the co-facial co-conformations at lower temperatures. Although in solution the rotaxane components are free to rotate and can still adopt many different co-conformations, it is not unreasonable to expect

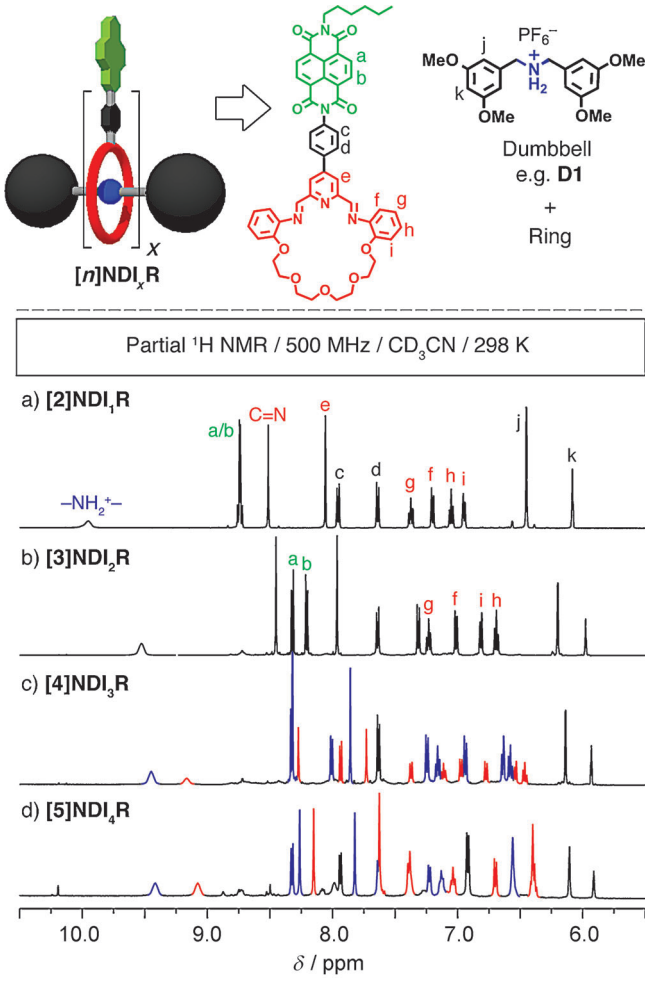


***Figure 1.*** Partial $^1$H NMR spectra (500 MHz/CD$_3$CN/298 K) of the ***[n]*NDI$_x$R** series. The resonances for the NDI protons $H_a$ and $H_b$ separate and shift significantly upfield as the number of rings is increased from one to two in a) **[2]NDI$_1$R** and b) **[3]NDI$_2$R**, respectively, an indication of the existence of π–π interactions between the NDI units. Two sets of resonances occurring in c) 2:1 and d) 1:1 ratios are consistent with the constitutionally heterotopic nature of the outer (blue signals) and inner (red signals) rings of the [4]- and [5]rotaxanes **[4]NDI$_3$R** and **[5]NDI$_4$R**, respectively.

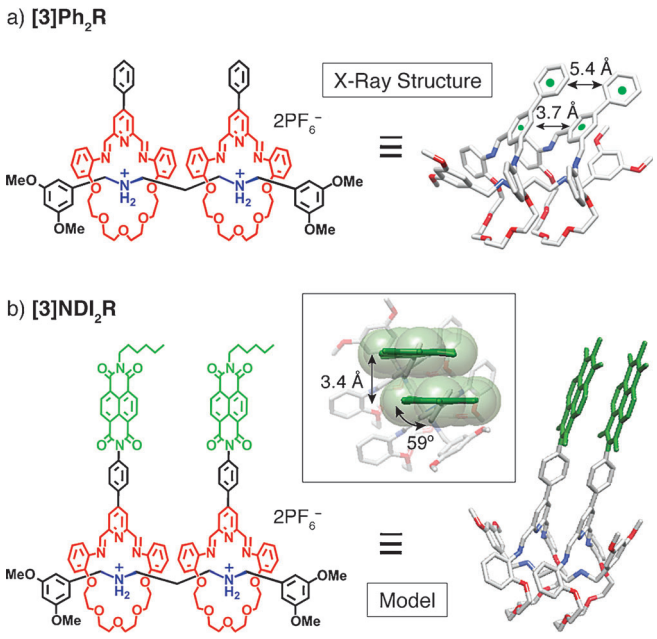


***Figure 2.*** a) Structural formula and single-crystal X-ray structure of the related [3]rotaxane **[3]Ph$_2$R**. Hydrogen atoms have been omitted for the sake of clarity. The solid-state structure of **[3]Ph$_2$R** shows a co-facial arrangement of the phenyl groups yet negligible π–π interactions as a consequence of the slipped-stack relationship between the rings which creates a 5.4 Å centroid-to-centroid distance between them. b) Structural formula and graphical representation of the DFT-calculated (B3LYP-D3/6-31G**) geometry-optimized structure of **[3]NDI$_2$R**, which was constructed from the solid-state structure obtained for **[3]Ph$_2$R**. Inset: A plan view of the geometry-optimized structure of **[3]NDI$_2$R** superimposed upon the corresponding space-filling representation depicting 1) a 59° twist between the NDI units and phenylene rings and 2) the two co-facial NDI units at a 3.4 Å plane-to-plane distance apart.

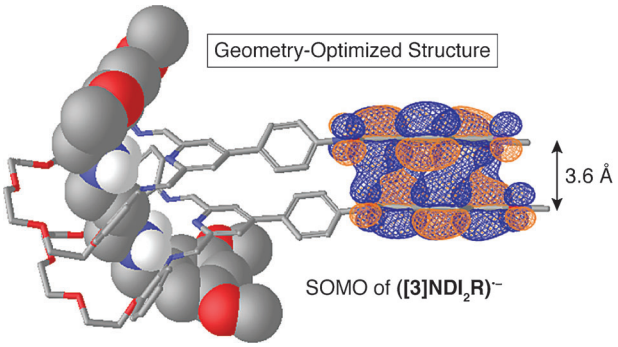


***Figure 3.*** Graphical representation of the DFT-calculated (B3LYP-D3/6-31G** level of theory) singly occupied molecular orbital (SOMO) of **([3]NDI$_2$R)$^{\bullet-}$**. Orbital isosurfaces are illustrated at 0.015 electrons Bohr$^{-1}$.

the proximate NDI units to favor co-facial π-interactions based on the available data.[23,24,26]

In order to examine the interactions between the NDI units in the **[*n*]NDI$_x$R** series, we directed our attention towards investigating their redox properties by cyclic voltammetry (CV) in solution. We also performed CV experiments (Supporting Information, Figure S28) on **1-NDI** and the control compound **3** to probe the effects of the mechanical bond on the reduction potential of the NDI units. The [2]rotaxane (Figure S29) **[2]NDI$_1$R** exhibits two one-electron reductions at −0.73 and −1.20 V corresponding[19,20] to the generation of **NDI$^{\bullet-}$** and **NDI$^{2-}$**, respectively. On scanning at even more negative potentials, a third one-electron process is observed at −1.44 V. This redox process is also evident in the CV of **1-NDI**, but not in the control **3**, leading us to associate this feature with the reduction of the pyridine ring.[27] Figure 4, which illustrates the first-wave reductions of the **[*n*]NDI$_x$R** series of oligorotaxanes, reveals a separation of the first one-electron process observed (Figure 4a) in the case of **[2]NDI$_1$R** into ***x*** discrete one-electron steps as a result of the electronic communication between the NDI units in the arrays as the number of NDI units is increased. The first reduction (−0.67 V) of **[3]NDI$_2$R** is easier to perform (Figure 4b) than that (−0.73 V) of **[2]NDI$_1$R** owing to the favorable interactions between the two electron-deficient NDI units. On the other hand, the fact that the second NDI reduction (−0.88 V) of **[3]NDI$_2$R** to is more difficult to achieve on account of the destabilizing interactions present in the electron-rich system. Similar trends are observed (Figure 4c) for **[4]NDI$_3$R** where three reductions (−0.59, −0.73, and −0.85 V) are observed for the generation one, two, and three **NDI$^{\bullet-}$** in the [4]rotaxane, respectively. Indeed, the NDI geometries and rotaxane co-conformations adopted by **[5]NDI$_4$R** become increasingly more complex and less well-defined (Figure 4d) as it is reduced at −0.57 V down to −0.97 V from the mono-reduced species to the tetra-anion. Nevertheless, in each of these examples, the emergence of ***x*** discrete redox processes suggests that, even when up to four electrons are introduced into an array like **[5]NDI$_4$R**, communication between the NDI units is preserved despite the potential for unfavorable charge repulsion to occur.

Electron paramagnetic resonance (EPR) spectroscopy at X-band (9.5 GHz) was used to explore (Figure 5) electron sharing within the singly reduced **([*n*]NDI$_x$R)$^{\bullet-}$** series at 270 K. Specifically, if an electron is being shared across identical NDI monomers on the timescale of the **NDI$^{\bullet-}$** monomer electron-nuclear hyperfine couplings (ca. $10^7$ s$^{-1}$), then a narrowing of the spectral width proportional to the square root of the number of monomers should be observed.[28] Although this spectral narrowing was not observed for **([3]NDI$_2$R)$^{\bullet-}$** when compared with **([2]NDI$_1$R)$^{\bullet-}$** and the control **3$^{\bullet-}$**, partial narrowing is apparent in the spectra of **([4]NDI$_3$R)$^{\bullet-}$** and **([5]NDI$_4$R)$^{\bullet-}$**. The EPR spectra (Figure 5) of **([*n*]NDI$_x$R)$^{\bullet-}$** at 270 K in

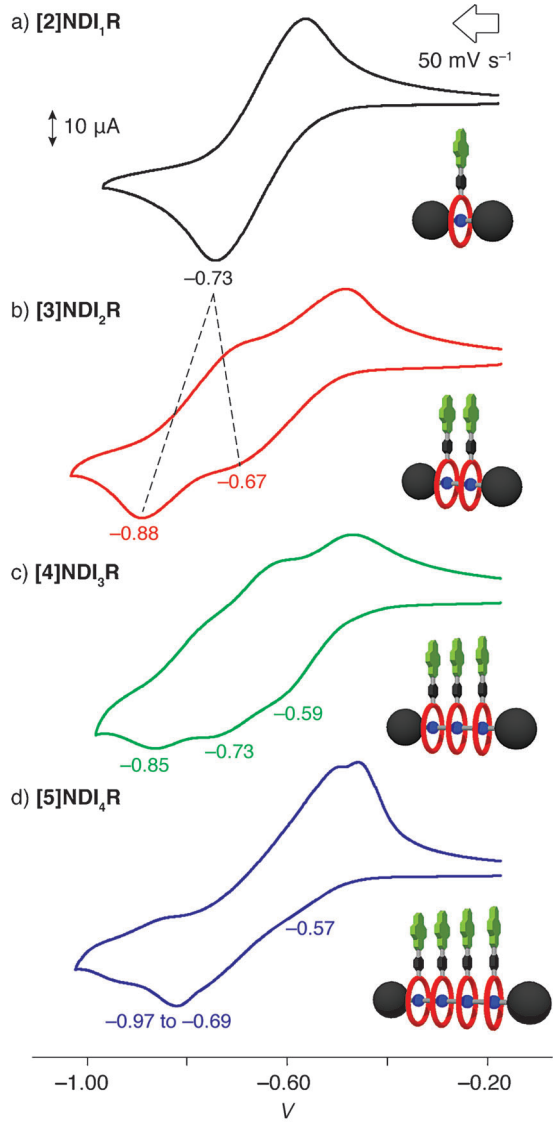


***Figure 4.*** Cyclic voltammograms (CVs) of the **[*n*]NDI$_x$R** series (scan rate 50 mV s$^{-1}$) depicting successive first-electron reductions of one, two, three, and four NDI units in a) [2]-, b) [3]-, c) [4]-, and d) [5]rotaxanes, respectively. All the experiments were performed at 298 K in Ar-purged $CH_2Cl_2$ solutions (1.0 mM) with 0.1 M $TBAPF_6$ as the supporting electrolyte. The splitting of first-wave reductions into ***x*** one-electron steps is a clear indication of electronic coupling between NDI units in the arrays.

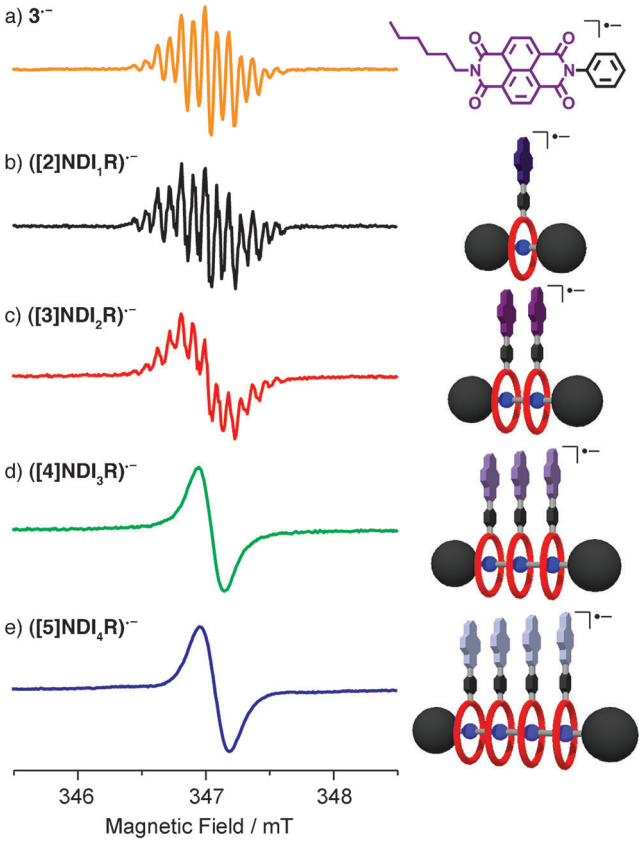


***Figure 5.*** EPR Spectra of a) **3**$^{\bullet-}$ and b–e) the **([*n*]NDI$_x$R)**$^{\bullet-}$ series after reduction with 1.0 equiv of $CoCp_2$. All spectra were recorded in Ar-purged $CH_2Cl_2$ solutions (0.75 mM) at 270 K at X-band (9.5 GHz) with 0.020 mT modulation amplitude. The hyperfine splitting of b) **([2]NDI$_1$R)**$^{\bullet-}$ and c) **([3]NDI$_2$R)**$^{\bullet-}$ remain partially resolved, whereas the spectra for d) **([4]NDI$_3$R)**$^{\bullet-}$ and e) **([5]NDI$_4$R)**$^{\bullet-}$ reveal a featureless signal. Inhomogenous broadening of the EPR spectra relative to (a) monomeric NDI **3** is attributed to the slower molecular tumbling rate of the larger oligorotaxanes.

$CH_2Cl_2$ are inhomogenously broadened relative (Figure 5a) to the control **3**$^{\bullet-}$ because of the slower molecular tumbling rates for the larger compounds, as well as a loss in resolution of the hyperfine splitting resulting from electron sharing, except for the spectra (Figure 5b,c) of **([2]NDI$_1$R)**$^{\bullet-}$ and **([3]NDI$_2$R)**$^{\bullet-}$ in which the hyperfine splittings are still partially resolved. The spectra (Figure 5d,e) of **([4]NDI$_3$R)**$^{\bullet-}$ and **([5]NDI$_4$R)**$^{\bullet-}$ exhibit a single unresolved line. The lack of significant spectral narrowing in the case of **([3]NDI$_2$R)**$^{\bullet-}$ led us to hypothesize that there are a number of internal nuclear reorganization events—such as intramolecular rotation of the ring around the dumbbell inducing NDI motion—which create a high barrier to electron sharing on the timescale of the EPR experiment. We attempted to limit intramolecular motions by lowering the temperature of **([3]NDI$_2$R)**$^{\bullet-}$ to 200 K; however, no change in EPR linewidth was observed (Figure S30). For the remaining oligorotaxanes, linewidth analysis using Equation (1) in Ref. [28] gives values for $N_S$ of 2.21 and 1.83 for **([4]NDI$_3$R)**$^{\bullet-}$ and **([5]NDI$_4$R)**$^{\bullet-}$, respectively, providing conclusive evidence that, although the electron can be shared across these higher order rotaxanes on this timescale, perfect sharing is likely to be hindered by the distribution of different co-conformations.

Continuous-wave electron-nuclear double resonance (ENDOR) spectroscopy (Figure 6) allows for the detection of unresolved hyperfine couplings in the EPR spectra of radicals,[29] thus providing higher resolution data on electron sharing. On account of the flexible nature of the NDIs in the oligorotaxanes, we hypothesized that a larger extent of electron sharing might be observable with ENDOR spectroscopy. Isotropic hyperfine coupling constants (hfccs) for the singly reduced **([*n*]NDI$_x$R)**$^{\bullet-}$ series were measured in $CH_2Cl_2$ at 270 K (Table 1) and follow the resonance condition $\nu^{\pm}_{ENDOR} = |\nu_n \pm (a_H/2)|$, where $\nu^{\pm}_{ENDOR}$ is the ENDOR transition frequency and $\nu_n$ is the proton Larmor frequency. The ENDOR spectrum (Figure 6b) of **([2]NDI$_1$R)**$^{\bullet-}$ shows the expected ENDOR signal consistent with previously assigned spectra of **NDI**$^{\bullet-}$ derivatives with an unsubstituted core.[19,30] The ENDOR spectrum (Figure 6c) of **([3]NDI$_2$R)**$^{\bullet-}$ shows a near-perfect one-half reduction of the hfccs established by **([2]NDI$_1$R)**$^{\bullet-}$ compared to those calculated for the asymmetrically substituted control **3**$^{\bullet-}$. This observation provides conclusive evidence that the unpaired electron is being fully shared across two NDI units on a timescale $\geq 10^7\ s^{-1}$. The ENDOR spectra (Figure 6d,e) of **([4]NDI$_3$R)**$^{\bullet-}$ and **([5]NDI$_4$R)**$^{\bullet-}$ appear to exhibit fractional sharing in which the broader linewidths provide evidence of several populations that we suspect arise from dynamic motions taking place between the NDI units and the partial disruption of π-orbital overlap. The spectra, however, are narrowed still further as a result of the increased probability that any two NDI units

***Table 1:*** Hyperfine coupling constants (hfccs) obtained from electron-nuclear double resonance (ENDOR) spectra.

| Compound | Hyperfine coupling constants[a] (hfccs) [MHz] | | |
|---|---|---|---|
| **3**$^{\bullet-}$ (theor.)[b] | 5.27 | 4.84 | 0.75 |
| **3**$^{\bullet-}$ (expt.) | 5.34 | – | 0.43 |
| **([2]NDI$_1$R)**$^{\bullet-}$[c,d] | 5.85 | 4.76 | 0.56 |
| **([3]NDI$_2$R)**$^{\bullet-}$[c,e] | 3.05 | 2.49 | 0.28 |
| **([4]NDI$_3$R)**$^{\bullet-}$[f] | 3.82 | 3.11 | 0.90 |
| **([5]NDI$_4$R)**$^{\bullet-}$[f] | 2.39 | – | 1.02 |

[a] hfcc values reflect coupling of the unpaired electron to either the asymmetric protons on the NDI core or the sp$^3$ hybridized methylene protons nearest the imide nitrogen atom. Calculations show that the naphthalene protons closest to the phenyl substituent are more strongly coupled, that is, exhibit higher hfccs, than those protons near the hexyl chain. [b] Theoretical hfccs for the control **3**$^{\bullet-}$ were calculated at the UB3LYP/EPR-II level of theory. [c] The differences in hfccs are resolved for molecules **([2]NDI$_1$R)**$^{\bullet-}$ and **([3]NDI$_2$R)**$^{\bullet-}$. The weaker hyperfine coupling constant observed below 1.0 MHz is a result of the interactions between the unpaired electron and the protons of the methylene nearest the imide nitrogen atom. [d] The experimental hfccs determined for **([2]NDI$_1$R)**$^{\bullet-}$ are in agreement with the theoretical and experimental hfccs recorded for the control **3**$^{\bullet-}$. [e] Reduction of all hfccs for **([3]NDI$_2$R)**$^{\bullet-}$ relative to **([2]NDI$_1$R)**$^{\bullet-}$ by a factor of two demonstrates sharing of the electron between two identical NDI units in the [3]rotaxane. [f] Although substantial reduction of the hfccs is also apparent for **([4]NDI$_3$R)**$^{\bullet-}$ and **([5]NDI$_4$R)**$^{\bullet-}$, the extent of electron sharing (or efficiency of π-orbital overlap) between the NDI units is ultimately impacted by the various NDI geometries and rotaxane co-conformations that can be adopted, which makes it difficult to assign the 0.90 and 1.02 MHz couplings.

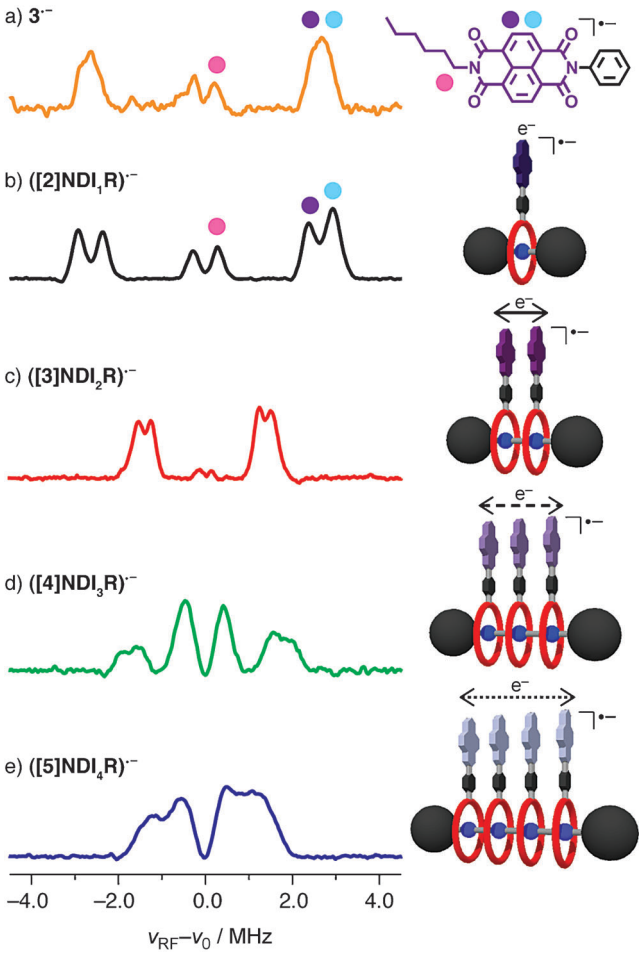


***Figure 6.*** ENDOR Spectroscopy of a) **3**$^{\bullet-}$ and b–e) the **([*n*]NDI$_x$R)**$^{\bullet-}$ series after reduction with 1.0 equiv of $CoCp_2$ provides conclusive evidence for electron sharing between the NDI units in the linear oligorotaxane arrays. All spectra were recorded in Ar-purged $CH_2Cl_2$ solutions (0.75 mM) at 270 K. The proton Larmor frequency is indicated by $\nu_0$. The near-perfect one-half reduction of the proton-hyperfine interactions in c) **([3]NDI$_2$R)**$^{\bullet-}$ confirms that the electron is being shared fully across the two NDI units on the ENDOR timescale. The ENDOR spectra of d) **([4]NDI$_3$R)**$^{\bullet-}$ and e) **([5]NDI$_4$R)**$^{\bullet-}$ reveal fractional sharing of the unpaired electrons and the existence of different populations, most likely as a consequence of the dynamic π–π interactions between three and four NDI units in the arrays, respectively.

are within a favorable geometry for electron sharing to occur. In short, the ENDOR data suggests that, while each and every NDI unit in the array is involved in mediating an electron through the array, their π-orbitals may not be perfectly aligned into active electron sharing domains at all times. This idea is consistent with previous reports in the literature[31] on non-mechanically interlocked assemblies where electron sharing is only observed to occur through a fraction of the system and can be attributed to the concept of *conformational gating*.[32] In this case, electron sharing is mediated by the thermally driven intramolecular motions which enable the alignment of NDI π-orbitals within the oligorotaxane. Indeed, the degree of π-orbital overlap between co-facial NDI units could be limited certainly by the slipped-stacked and twisted nature of NDI units on the ring, leading to imperfect stacking. Furthermore, the flexible nature of the rotaxane components resulting from the mechanical bond enables other modes of disorder.

In summary, we have demonstrated through-space electron sharing in a series of mechanically interlocked molecules featuring single-molecular 1D arrays of NDIs, capable of forming co-facial stacks. In contrast with previous approaches to preparing through-space molecular wires where non-trivial syntheses and uncontrolled assembly of molecular components can limit the size of a system and produce ambiguous results, we have been able to control sequentially 1) the number of NDI units and 2) their relative dispositions employing a template-assisted strategy and mechanical bonding. As a result, we have been able to show in a systematic fashion the through-space delocalization of an electron through co-facial stacks of NDIs with only a moderate loss in transport as the length of the array is increased. The present data suggests that the electron sharing process is conformationally gated by the relative motions of NDI units within the stack as a consequence of the mechanical bond, which allows individual rotaxane components to move in and out of active electron sharing domains. Strategies to attenuate and control these degrees of freedom in order to elucidate and improve electron transport in these materials are currently in progress in our laboratories. These experimental results demonstrate the untapped utility of mechanically interlocked molecules in constructing functional organic motifs, which may serve to enhance our understanding of organic electronics in the future.

Received: November 6, 2013
Published online: March 12, 2014

**Keywords:** electron transport · mechanically interlocked molecules · radical anions · self-assembly · template-directed synthesis

[1] a) D. Gust, T. A. Moore, A. L. Moore, *Acc. Chem. Res.* **1993**, *26*, 198–205; b) C. J. Murphy, M. R. Arkin, Y. Jenkins, N. D. Ghatlia, S. H. Bossmann, N. J. Turro, J. K. Barton, *Science* **1993**, *262*, 1025–1029; c) J. C. Genereux, J. K. Barton, *Chem. Rev.* **2010**, *110*, 1642–1662.

[2] a) M. R. Wasielewski, *Acc. Chem. Res.* **2009**, *42*, 1910–1921; b) R. Bhosale, J. Mišek, N. Sakai, S. Matile, *Chem. Soc. Rev.* **2010**, *39*, 138–149; c) F. Garo, R. Häner, *Angew. Chem.* **2012**, *124*, 940–943; *Angew. Chem. Int. Ed.* **2012**, *51*, 916–919; d) P. Frischmann, K. Mahata, F. Würthner, *Chem. Soc. Rev.* **2013**, *42*, 1847–1870; e) G. Sforazzini, E. Orentas, A. Bolag, N. Sakai, S. Matile, *J. Am. Chem. Soc.* **2013**, *135*, 12082–12090.

[3] a) A. Takai, T. Yasuda, T. Ishizuka, T. Kojima, M. Takeuchi, *Angew. Chem.* **2013**, *125*, 9337–9341; *Angew. Chem. Int. Ed.* **2013**, *52*, 9167–9171; b) A. C. Fahrenbach, S. C. Warren, J. T. Incorvati, A.-J. Avestro, J. C. Barnes, J. F. Stoddart, B. A. Grzybowski, *Adv. Mater.* **2013**, *25*, 331–348.

[4] a) V. Percec, M. Glodde, T. K. Bera, Y. Miura, I. Shiyanovskaya, K. D. Singer, V. S. K. Balagurusamy, P. A. Heiney, I. Schnell, A. Rapp, H.-W. Spiess, S. D. Hudson, H. Duan, *Nature* **2002**, *417*, 384–387; b) T. Aida, E. W. Meijer, S. I. Stupp, *Science* **2012**, *335*, 813–817; c) H. Usta, M. D. Yilmaz, A.-J. Avestro, D. Boudinet,

M. Denti, J. F. Stoddart, A. Facchetti, *Adv. Mater.* **2013**, *25*, 4327 – 4334.

[5] a) W. B. Davis, W. A. Svec, M. A. Ratner, M. R. Wasielewski, *Nature* **1998**, *396*, 60 – 63; b) C. A. Hunter, S. Tomas, *J. Am. Chem. Soc.* **2006**, *128*, 8975 – 8979; c) P. M. Beaujuge, J. M. J. Fréchet, *J. Am. Chem. Soc.* **2011**, *133*, 20009 – 20029; d) A. Coskun, J. M. Spruell, G. Barin, W. R. Dichtel, A. H. Flood, Y. Y. Botros, J. F. Stoddart, *Chem. Soc. Rev.* **2012**, *41*, 4827 – 4859.

[6] a) H. Oevering, M. N. Paddon-Row, M. Heppener, A. M. Oliver, E. Cotsaris, J. W. Verhoeven, N. S. Hush, *J. Am. Chem. Soc.* **1987**, *109*, 3258 – 3269; b) E. A. Weiss, M. J. Ahrens, L. E. Sinks, A. V. Gusev, M. A. Ratner, M. R. Wasielewski, *J. Am. Chem. Soc.* **2004**, *126*, 5577 – 5584; c) M. Scott, T. Miura, A. Butler Ricks, Z. E. X. Dance, E. M. Giacobbe, M. T. Colvin, M. R. Wasielewski, *J. Am. Chem. Soc.* **2009**, *131*, 17655 – 17666.

[7] a) F.-R. F. Fan, J. Yang, L. Cai, D. W. Price, Jr., S. M. Dirk, D. V. Kosynkin, Y. Yao, A. M. Rawlett, J. M. Tour, A. J. Bard, *J. Am. Chem. Soc.* **2002**, *124*, 5550 – 5560; b) S. A. Serron, S. A. Aldridge III, C. N. Fleming, R. M. Danell, M.-H. Bailk, M. Sykora, D. M. Dettelbaum, T. J. Meyer, *J. Am. Chem. Soc.* **2004**, *126*, 14506 – 14514; c) T. M. Wilson, T. A. Zeidan, M. Hariharan, F. D. Lewis, M. R. Wasielewski, *Angew. Chem.* **2010**, *122*, 2435 – 2438; *Angew. Chem. Int. Ed.* **2010**, *49*, 2385 – 2388; d) S. Sengupta, D. Ebeling, S. Patwardhan, X. Zhang, H. von Berlepsch, C. Böttcher, V. Stepanenko, S. Uemura, C. Hentschel, H. Fuchs, F. C. Grozema, L. D. A. Siebbeles, A. R. Holzwarth, L. Chi, F. Würthner, *Angew. Chem.* **2012**, *124*, 6484 – 6488; *Angew. Chem. Int. Ed.* **2012**, *51*, 6378 – 6382.

[8] a) Y. Morisaki, S. Ueno, A. Saeki, A. Asano, S. Seki, Y. Chujo, *Chem. Eur. J.* **2012**, *18*, 4216 – 4224; b) M. Wielopolski, A. Molina-Ontoria, C. Schubert, J. T. Margraf, E. Krokos, J. Kirschner, A. Gouloumis, T. Clark, D. M. Guldi, N. Martin, *J. Am. Chem. Soc.* **2013**, *135*, 10372 – 10381.

[9] J. E. Bullock, R. Carmieli, S. M. Mickley, J. Vura-Weis, M. R. Wasielewski, *J. Am. Chem. Soc.* **2009**, *131*, 11919 – 11929.

[10] a) S. Anderson, H. L. Anderson, J. K. M. Sanders, *Acc. Chem. Res.* **1993**, *26*, 469 – 475; b) R. Cacciapaglia, L. Manodolini, *Chem. Soc. Rev.* **1993**, *22*, 221 – 231; c) R. Hoss, F. Vögtle, *Angew. Chem.* **1994**, *106*, 389 – 398; *Angew. Chem. Int. Ed. Engl.* **1994**, *33*, 375 – 384; d) G. A. Breault, C. A. Hunter, P. C. Mayers, *Tetrahedron* **1999**, *55*, 5265 – 5293; e) T. J. Hubin, D. H. Busch, *Coord. Chem. Rev.* **2000**, *200*, 5 – 52; f) M.-J. Blanco, J.-C. Chambron, M. C. Jiménez, J.-P. Sauvage, *Top. Stereochem.* **2002**, *23*, 125 – 173; g) D. H. Busch, *Top. Curr. Chem.* **2005**, *249*, 1 – 65; h) C. D. Meyer, C. S. Joiner, J. F. Stoddart, *Chem. Soc. Rev.* **2007**, *36*, 1705 – 1723.

[11] a) T. R. Kelly, R. L. Xie, C. K. Weinreb, T. Bregant, *Tetrahedron Lett.* **1998**, *39*, 3675 – 3678; b) Y. Xia, P. Yang, Y. Sun, Y. Wu, B. Mayers, B. Gates, Y. Yin, F. Kim, H. Yan, *Adv. Mater.* **2003**, *15*, 353 – 389; c) L. Palmer, S. I. Stupp, *Acc. Chem. Res.* **2008**, *41*, 1674 – 1684.

[12] Y.-L. Wu, K. E. Brown, M. R. Wasielewski, *J. Am. Chem. Soc.* **2013**, *135*, 13322 – 13325.

[13] a) N. Sakai, M. Lista, O. Kel, S. Sakurai, D. Emery, J. Mareda, E. Vauthey, S. Matile, *J. Am. Chem. Soc.* **2011**, *133*, 15224 – 15227; b) M. Lista, J. Areephong, N. Sakai, S. Matile, *J. Am. Chem. Soc.* **2011**, *133*, 15228 – 15230; c) N. Sakai, S. Matile, *J. Am. Chem. Soc.* **2011**, *133*, 18542 – 18545.

[14] a) Y. Yamauchi, M. Yoshizawa, M. Akita, M. Fujita, *J. Am. Chem. Soc.* **2010**, *132*, 960 – 966; b) M. Kiguchi, T. Takahashi, Y. Takahashi, Y. Yamauchi, T. Murase, M. Fujita, T. Tada, S. Watanabe, *Angew. Chem.* **2011**, *123*, 5826 – 5829; *Angew. Chem. Int. Ed.* **2011**, *50*, 5708 – 5711.

[15] M. Kiguchi, O. Tal, S. Wohlthat, F. Pauly, M. Krieger, D. Djukic, J. C. Cueves, J. M. van Ruitenbeek, *Phys. Rev. Lett.* **2008**, *101*, 046801.

[16] a) P. T. Glink, A. I. Oliva, J. F. Stoddart, A. J. P. White, D. J. Williams, *Angew. Chem.* **2001**, *113*, 1922 – 1927; *Angew. Chem. Int. Ed.* **2001**, *40*, 1870 – 1875; b) M. Horn, J. Ihringer, P. T. Glink, J. F. Stoddart, *Chem. Eur. J.* **2003**, *9*, 4046 – 4054.

[17] a) S. J. Rowan, S. J. Cantrill, G. R. L. Cousins, J. K. M. Sanders, J. F. Stoddart, *Angew. Chem.* **2002**, *114*, 938 – 993; *Angew. Chem. Int. Ed.* **2002**, *41*, 898 – 952; b) J. M. Lehn, *Chem. Soc. Rev.* **2007**, *36*, 151 – 160; c) M. E. Belowich, J. F. Stoddart, *Chem. Soc. Rev.* **2012**, *41*, 2003 – 2024; d) Y. Jin, C. Yu, R. J. Denman, W. Zhang, *Chem. Soc. Rev.* **2013**, *42*, 6634 – 6654.

[18] a) M. E. Belowich, C. Valente, R. A. Smaldone, D. C. Friedman, J. Thiel, L. Cronin, J. F. Stoddart, *J. Am. Chem. Soc.* **2012**, *134*, 5243 – 5261; b) A.-J. Avestro, M. E. Belowich, J. F. Stoddart, *Chem. Soc. Rev.* **2012**, *41*, 5869 – 6216.

[19] a) S. C. Bhosale, S. V. Bhosale, S. K. Bhargava, *Org. Biomol. Chem.* **2012**, *10*, 6455 – 6468; b) Z. Zhu, C. J. Cardin, Y. Gan, H. M. Colquhoun, *Nat. Chem.* **2010**, *2*, 653 – 660; c) A. Das, S. Ghosh, *Macromolecules* **2013**, *46*, 3939 – 3949; d) M. B. Avinash, T. Govindaraju, *Adv. Mater.* **2012**, *24*, 3905 – 3922; e) M. B. Avinash, E. Verheggen, C. Schmuck, T. Govindaraju, *Angew. Chem.* **2012**, *124*, 10470 – 10474; *Angew. Chem. Int. Ed.* **2012**, *51*, 10324 – 10328; f) R. S. Lokey, Y. Kwok, V. Guelev, C. J. Pursell, L. H. Hurley, B. L. Iverson, *J. Am. Chem. Soc.* **1997**, *119*, 7202 – 7210; g) A. R. Smith, B. L. Iverson, *J. Am. Chem. Soc.* **2013**, *1035*, 12783 – 12789; h) S. V. Bhosale, C. H. Jani, S. J. Langford, *Chem. Soc. Rev.* **2008**, *37*, 331 – 342; i) N. Sakai, J. Mareda, E. Vauthey, S. Matile, *Chem. Commun.* **2010**, *46*, 4225 – 4237; j) S. Tu, S. H. Kim, J. Joseph, D. A. Modarelli, J. R. Parquette, *ChemPhysChem* **2013**, *14*, 1609 – 1617; k) H. Shao, T. Nguyen, N. C. Romano, D. A. Modarelli, J. R. Parquette, *J. Am. Chem. Soc.* **2009**, *131*, 16374 – 16376; l) S. Guha, F. S. Goodson, S. Roy, L. J. Corson, C. A. Gravenmier, S. Saha, *J. Am. Chem. Soc.* **2011**, *133*, 15256 – 15259; m) N. Ponnuswamy, F. B. L. Cougnon, J. M. Clough, G. D. Pantoş, J. K. M. Sanders, *Science* **2012**, *338*, 783 – 785; n) S. P. Black, A. R. Stefankiewicz, M. M. J. Smulders, D. Sattler, C. A. Schalley, J. R. Nitschke, J. K. M. Sanders, *Angew. Chem.* **2013**, *125*, 5861 – 5864; *Angew. Chem. Int. Ed.* **2013**, *52*, 5749 – 5752; o) C. Shao, M. Stolte, F. Würthner, *Angew. Chem.* **2013**, *125*, 7630 – 7634; *Angew. Chem. Int. Ed.* **2013**, *52*, 7482 – 7486; p) S. Sengupta, F. Würthner, *Acc. Chem. Res.* **2013**, *46*, 2498 – 2512; q) Y. S. Chong, W. R. Carroll, W. G. Burns, M. D. Smith, K. D. Shimizu, *Chem. Eur. J.* **2009**, *15*, 9117 – 9126; r) X. Guo, D. Zhang, D. Zhu, *Adv. Mater.* **2004**, *16*, 125 – 130.

[20] X. Zhan, A. Facchetti, S. Barlow, T. J. Marks, M. A. Ratner, M. R. Wasielewski, S. R. Marder, *Adv. Mater.* **2011**, *23*, 268 – 284.

[21] The peak integrations are consistent with the ratios of the constitutionally heterotopic outer and inner rings (blue and red in the $^1$H NMR spectra) present in the **[*n*]NDI$_x$R** series—that is, 2:1 and 1:1 for $x = 3$ and 4, respectively.

[22] All efforts resulted in single crystals that were either twinned or unable to diffract with high enough resolution. The ability of the rings to rotate or twist around the dumbbells in order to accommodate the sterically bulky groups could result conceivably in multiple favorable co-conformations in the solid state. Surprisingly, out of the entire **[*n*]NDI$_x$R** series, the most successful crystallizations were achieved from solutions (0.9 mg mL$^{-1}$) of **[5]NDI$_4$R** in $CH_2Cl_2$/*n*-heptane grown at 0 °C, yet these crystals were only able to diffract up to 2.8 Å using a Cu beam source. We attribute this observation to the more rigid structure afforded by multiple interactions when $x = 4$.

[23] Crystal data for the [3]rotaxane **[3]Ph$_2$R**: $C_{95}H_{109}F_{12}N_9O_{14}P_2$, MW = 1890.891, monoclinic, space group $P1n1$, $a$ = 24.5464(18), $b$ = 15.2507(10), $c$ = 25.4313(19) Å, $\beta$ = 95.403(5)°, $V$ = 9477.9(12) Å$^3$, $T$ = 100(2) K, $Z$ = 4, $\rho_{calc}$ = 1.325 g cm$^{-3}$, $\mu$(Cu-K$\alpha$) = 1.188, $F(000)$ = 3968. Independent measured reflections 16367. $R1$ = 0.1117, $wR2$ = 0.3415 for 9167 independent observed reflections [$2\theta \le 57.62°$, $I > 2\sigma(I)$]. CCDC 963939

  

([**3]Ph$_2$R**) contains the supplementary crystallographic data for this paper. These data can be obtained free of charge from The Cambridge Crystallographic Data Centre via www.ccdc.cam.ac.uk/data_request/cif.

[24] The computed structure of **[3]NDI$_2$R** was obtained by modeling the NDI units directly onto the X-ray crystal structure obtained for the related [3]rotaxane **[3]Ph$_2$R** (see Ref. [23]), which is devoid of the NDI functionality, and performing an unconstrained geometry optimization at the B3LYP-D3/6-31G** level of theory (Ref. [25]). Density functional theory (DFT) measurements were only carried out on the [2]rotaxane **[3]NDI$_2$R** since calculations on the higher order [*n*]rotaxanes failed to converge in a reasonable amount of time.

[25] a) C. Lee, W. Yang, R. G. Parr, *Phys. Rev. B* **1988**, *37*, 785 – 789; b) A. D. Becke, *J. Chem. Phys.* **1993**, *98*, 1372 – 1377; c) S. Grimme, J. Antony, S. Ehrlich, H. Krieg, *J. Chem. Phys.* **2010**, *132*, 154104.

[26] UV/Vis spectroscopy (Figure S27) of the **[*n*]NDI$_x$R** series (5.0 μM in $CH_2Cl_2$) reveals the existence of three absorption bands between 330 and 400 nm characteristic of other NDI derivatives in the literature (Ref. [19]). An intensity reversal of the absorptions centered at 360 and 380 nm, relative to one another as the number of NDI units is increased, may indicate weak exciton coupling between the NDI units in the [*n*]rotaxanes in $CH_2Cl_2$ solution. For more details, see: a) M. Kasha, H. R. Rawles, M. L. El-Bayoumi, *Pure Appl. Chem.* **1965**, *11*, 371 – 392; b) A. D. Q. Li, W. Wang, L. Q. Wang, *Chem. Eur. J.* **2003**, *9*, 4594 – 4601; c) J. M. Giaimo, J. V. Lockard, L. E. Sinks, A. M. Scott, T. M. Wilson, M. R. Wasielewski, *J. Phys. Chem. A* **2008**, *112*, 2322 – 2330.

[27] Since subjecting the [*n*]rotaxane samples (1.0 mM in Ar-purged $CH_2Cl_2$) to multiple redox cycles beyond −1.44 V resulted in decomposition of the molecules, presumably as a consequence of the irreversible reduction of the pyridine ring, applying high negative potentials were avoided when recording CV spectra. For more details, see: A. Cisak, P. J. Elving, *Electrochim. Acta* **1965**, *10*, 935 – 946.

[28] Sharing of an unpaired spin between identical monomeric units is characterized by narrowing of the EPR spectral linewidth by a factor proportional to the square root of the number of monomers involved, as given by Equation (1): $\Delta H_N = \left(1/\sqrt{N_S}\right)\Delta H_M$ which relates the linewidth of the monomer ($\Delta H_M$) to the observed linewidth ($\Delta H_N$) when an unpaired spin is shared over $N_S$ molecular sites. For more details, see: J. R. Norris, R. A. Uphaus, H. L. Crespi, J. J. Katz, *Proc. Natl. Acad. Sci. USA* **1971**, *68*, 625 – 628.

[29] H. Kurreck, B. Kirste, W. Lubitz, *Electron Nuclear Double Resonance Spectroscopy of Radicals in Solution*, VCH, New York, **1988**.

[30] a) J.-F. Penneau, B. J. Stallman, P. H. Kasai, L. L. Miller, *Chem. Mater.* **1991**, *3*, 791 – 796; b) L. L. Miller, R. G. Duan, Y. Hong, I. Tabakovic, *Chem. Mater.* **1995**, *7*, 1552 – 1557; c) L. L. Miller, K. R. Mann, *Acc. Chem. Res.* **1996**, *29*, 417 – 423.

[31] a) S. G. Chen, H. M. Branz, S. S. Eaton, P. C. Taylor, R. A. Cormier, B. A. Gregg, *J. Phys. Chem. B* **2004**, *108*, 17329 – 17336; b) Y. K. Che, A. Data, X. M. Yang, T. Naddo, J. C. Zhao, L. Zang, *J. Am. Chem. Soc.* **2007**, *129*, 6354 – 6355; c) T. M. Wilson, M. J. Tauber, M. R. Wasielewski, *J. Am. Chem. Soc.* **2009**, *131*, 8952 – 8957.

[32] The term "conformational gating" has been used to describe the thermally driven motion of base pairs to mediate hole transfer within double-stranded DNA. For more examples, see: a) G. I. Likhtenshtein, *J. Photochem. Photobiol. A* **1996**, *96*, 79 – 92; b) S. Delaney, J. K. Barton, *J. Org. Chem.* **2003**, *68*, 6475 – 6483; c) M. A. O'Neill, J. K. Barton, *J. Am. Chem. Soc.* **2004**, *126*, 11471 – 11483; d) E. A. Weiss, M. J. Tauber, R. F. Kelley, M. J. Ahrens, M. A. Ratner, M. R. Wasielewski, *J. Am. Chem. Soc.* **2005**, *127*, 11842 – 11850.

  